Physics 7230: Statistical Mechanics

Lecture Set 6: Quantum Many-Particle Statistical Mechanics

Leo Radzihovsky*

Department of Physics, University of Colorado, Boulder, CO 80309

(Dated: March 9, 2025)

Abstract

In this set of lectures, we will discuss quantum statistics of many particle systems. Focussing on bosons and fermions, as the only allowed statistics in three dimensions, we will apply quantum statistical mechanics to characterize low temperature properties of Bose and Fermi gases. The former will include applications to black- body radiation, phonons in solids and BEC and superfluidity. The latter will give us a description of metals, neutron stars, and will provide for a description of Pauli paramagnetism. In later lectures we will then apply ideas of exchange statistics to argue for the exchange interaction between spins in a crystal and will study ferromagnetism in solids.

*Electronic address: radzihov@colorado.edu

I. BASICS OF QUANTUM MANY-PARTICLE SYSTEMS IN 3D

- Degeneracy temperature T_*

  Quantum statistics of identical particles begins to manifest itself at low temperatures set by the degeneracy temperature

$$k_B T_* = \frac{\hbar^2 n^{2/3}}{2m},$$

  determined by purely by the density $n = 1/d^3$ of noninteracting quantum particles (d particle spacing), which sets their deBroglie wave-vector $k \sim n^{1/3}$, with $k_B T_*$ above the associated kinetic energy.

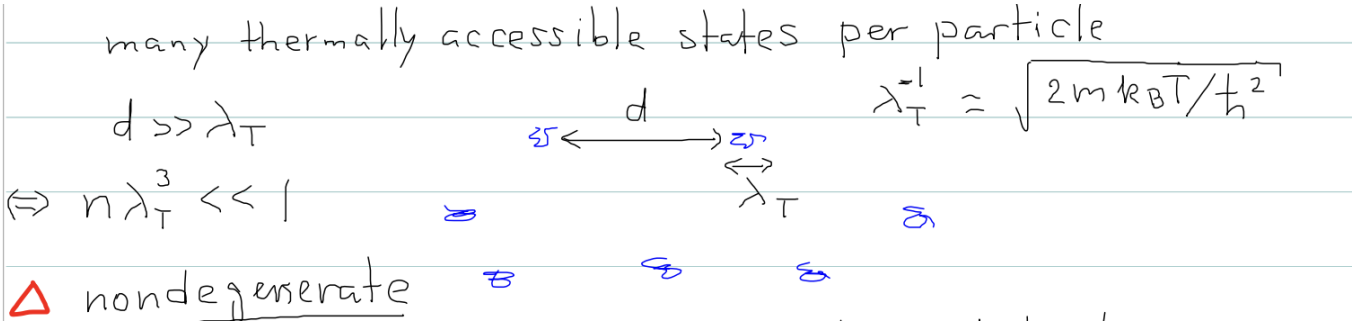

FIG. 1: Schematic illustration of nondegenerate regime of a gas of identical particles. It is defined by temperature above the degeneracy temperature, $T \gtrsim T_*$, or, equivalently thermal deBroglie wavelength smaller than the interparticle spacing,, $\lambda_T \lesssim 1/\sqrt{T} < d = n^{-1/3}$, or equivalently $n\lambda_T^3 \lesssim 1$.

- At high temperatures, $T \gtrsim T_*$, (or equivalently $n^{-1/3} = d \gtrsim \lambda_T$) quantum statistics of particles is irrelevant and any gas behaves like a Boltzmann classical gas.

- At low temperatures, $T \lesssim T_*$, (or equivalently $n^{-1/3} = d \lesssim \lambda_T$) quantum statistics of particles begins to manifest itself with drastic consequences. Recall we saw a hint of this from the unphysical result, $S_{\text{Boltzmann}}(T < T_*) < 0$.

- In 3D all particles fall into two quantum-statistically distinct classes, *bosons and fermions*, exhibiting vastically different phenomenology at low temperature $T \ll T_*$, or equivalently at high densities. In 2D can have more general quantum statistics of "anyons". In 1D statistics is not well defined as particles must interact to exchange.

– **Bosons**

* Examples: He^4, Li^7, K^{41} Rb^{87}... atoms (conserved bosonic matter); photons, Z, W (gauge bosons); phonons, excitons (bosonic excitations), and any particle composed of *even* number of fermions
* *Integer* spin, $s = 0, 1, 2, \ldots$ (spin-statistics theorem)
* *Even* under particle interchange,

$$\psi(\mathbf{r}_1, \mathbf{r}_2) = \psi(\mathbf{r}_2, \mathbf{r}_1) \equiv e^{i\theta}\psi(\mathbf{r}_2, \mathbf{r}_1), \ \theta = 0$$

* Unlimited number occupation $n_\alpha = 0, 1, 2, 3, \ldots$ of a single-particle states α.
*

$$q = \ln \mathcal{Z} = -\sum_\alpha \ln\left[1 - e^{-(\varepsilon_\alpha - \mu)/k_B T}\right], \quad n_\alpha^{\text{Bose-Einstein}} = \frac{1}{e^{(\varepsilon_\alpha - \mu)/k_B T} - 1}$$

* For $T < T_* \approx T_{\text{BEC}} \rightarrow$ Bose condensation ($\approx$ superfluidity, superconductivity, lasers), a macroscopic occupation of the lowest single particle state α.

– **Fermions**

* Examples: He^3, Li^6, K^{40} Rb^{84}... atoms, electrons, protons, neutrons, quarks, and any particle composed of *odd* number of fermions
* *Half-integer* spin, $s = 1/2, 3/2, 5/2, \ldots$ (spin-statistics theorem)
* *Odd* under particle interchange,

$$\psi(\mathbf{r}_1, \mathbf{r}_2) = -\psi(\mathbf{r}_2, \mathbf{r}_1) \equiv e^{i\theta}\psi(\mathbf{r}_2, \mathbf{r}_1), \ \theta = \pi$$

* Pauli Principle limited number occupation $n_\alpha = 0, 1$ of a single-particle state α.
*

$$q = \ln \mathcal{Z} = \sum_\alpha \ln\left[1 + e^{-(\varepsilon_\alpha - \mu)/k_B T}\right], \quad n_\alpha^{\text{Fermi-Dirac}} = \frac{1}{e^{(\varepsilon_\alpha - \mu)/k_B T} + 1}$$

* For $T < T_* \approx T_{\text{Fermi}} \rightarrow$ Fermi surface emerges, with quantum dynamics

confined to the vacinity of Fermi energy $E_F = \hbar^2 k_F^2/2m = k_B T_F$.

II. EXCHANGE STATISTICS AND MANY-PARTICLE WAVEFUNCTION

- **States of a noninteracting particles**

  Noninteracting particles are described by Hamiltonian $H = \sum_i H_i$ that decouples into a sum of single-particle Hamiltonians, H_i, with many-body eigenstates,

$$|E_{\{\alpha\}}\rangle = \prod_i^N |\varepsilon_{\alpha_i}\rangle, \quad E_{\{n_\alpha\}} = \sum_i^N \varepsilon_{\alpha_i} = \sum_\alpha n_\alpha \varepsilon_\alpha,$$

  defined by $H|E_{\{\alpha\}}\rangle = E_{\{\alpha\}}|E_{\{\alpha\}}\rangle$, a product of single particle eigenstates $|\varepsilon_\alpha\rangle$ and eigen-energies a sum of single particle eigen-energies ε_{α_i}, and we have also written many-body eigen-energies in terms of occupations n_α of α-th single-particle eigenstate, without any reference to a particle label i.

  In coordinate representation for *distinguishable* particles these are just product wavefunctions

$$\Psi^{\rm dist.}_{\{\alpha\}}(\{x_i\}) = \langle x_1, x_2, \ldots, x_N|\{\alpha\}\rangle = \prod_i^N \psi_{\alpha_i}(x_i). \tag{1}$$

  This decoupling is why the noninteracting N-body problem of distinguishable particles trivially reduces to N one-particle problems and is therefore easily solvable. Simple combinatorics gives us that there are $\frac{N!}{n_1! n_2! \ldots}$ distinct product states of the form $\Psi^{\rm dist.}_{\{\alpha\}}(\{x_i\})$. The naive Gibbs factor $1/N!$ attemps to adjust for identity of particles, giving

$$W_{\rm ClassicalGibbs} = \frac{1}{n_1! n_2! \ldots}.$$

  At high temperature, classical limit, when each single particle state α is rarely occupied, with $n_\alpha \ll 1$ on average, this Gibbs factor fix is sufficient. However, this clearly misses the low temperature regime, where α is multiply occupied, with n_α large.

  However, for quantum *indistinguishable* particles, even in the absence of interactions, quantum statistics plays a crucial role, making the problem nontrivial, though still exactly solvable. The key observation is that (1) is not a valid N-body state for N identical particles. The correct one must give observables, e.g., probability distribution

$|\Psi_{\{\alpha\}}|^2(x_1, x_2, \ldots, x_N)$, that is invariant under all particle interchanges $x_i \leftrightarrow x_j$, or equivalently under all elements of the permutation group, $P[\{x_i\}] = \{x_{Pi}\}$.

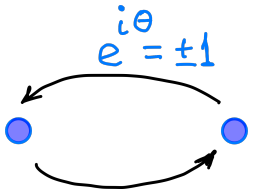

FIG. 2: Particle interchange characterized by statistical angle θ, that in 3D can only take on two values $\theta = 0, \pi$, respectively corresponding to bosons and fermions.

Thus, the *bosonic* choice of noninteracting N-particle wavefunction is given as a a *symmetric* sum over all permutations of set $\{i\}$ (or of $\{\alpha_i\}$) of product states in Eq.1, which can be written as a permanent of a matrix below,

$$\Psi^{\rm B}_{\alpha_1,\ldots,\alpha_N}(x_1, \ldots, x_N) \tag{2}$$

$$= \sqrt{\frac{n_1! n_2! \ldots}{N!}} \underbrace{[\psi_{\alpha_1}(x_1)\psi_{\alpha_2}(x_2)\ldots\psi_{\alpha_N}(x_N) + \psi_{\alpha_1}(x_{P1})\psi_{\alpha_2}(x_{P2})\ldots\psi_{\alpha_N}(x_{PN}) + \ldots]}_{\frac{N!}{n_1! n_2! \ldots} \textit{ distinct } \text{permutations}},$$

$$= \sqrt{\frac{1}{N! \prod_\alpha n_\alpha!}} \text{Permanent}\left[\psi_{\alpha_i}(x_j)\right], \quad \prod_\alpha n_\alpha! \text{ copies of } \frac{N!}{\prod_\alpha n_\alpha!} \text{ distinct terms},$$

$$= \sqrt{\frac{1}{N! \prod_\alpha n_\alpha!}} \text{Perm} \begin{bmatrix} \psi_{\alpha_1}(x_1) & \psi_{\alpha_1}(x_2) & \ldots & \psi_{\alpha_1}(x_N) \\ \psi_{\alpha_2}(x_1) & \psi_{\alpha_2}(x_2) & \ldots & \psi_{\alpha_2}(x_N) \\ \vdots & \ddots & & \\ \psi_{\alpha_N}(x_1) & \psi_{\alpha_N}(x_2) & \ldots & \psi_{\alpha_N}(x_N), \end{bmatrix} \tag{3}$$

with factors in front ensuring normalization.

For *fermions*, the N-particle wavefunction is an *antisymmetric* sum of permutations, i.e., with each permutation weighted by the signature of the permutation $(-1)^P$, which can be written as a determinant (called Slater determinant, after an eminent MIT physicist John Slater) of a matrix below,

$$\Psi^{\rm F}_{\alpha_1,\ldots,\alpha_N}(x_1,\ldots,x_N) \tag{4}$$
$$= \sqrt{\frac{n_1!n_2!\ldots}{N!}}\underbrace{\left[\psi_{\alpha_1}(x_1)\psi_{\alpha_2}(x_2)\ldots\psi_{\alpha_N}(x_N)+(-1)^P\psi_{\alpha_1}(x_{P1})\psi_{\alpha_2}(x_{P2})\ldots\psi_{\alpha_N}(x_{PN})+\ldots\right]}_{\frac{N!}{n_1!n_2!\ldots}\text{ permutations}},$$
$$= \sqrt{\frac{1}{N!\prod_\alpha n_\alpha!}}\text{Determinant}\left[\psi_{\alpha_i}(x_j)\right],\quad \prod_\alpha n_\alpha!\text{ copies of }\frac{N!}{\prod_\alpha n_\alpha!}\text{ distinct terms},$$
$$= \sqrt{\frac{1}{N!\prod_\alpha n_\alpha!}}\text{Det}\begin{bmatrix}\psi_{\alpha_1}(x_1) & \psi_{\alpha_1}(x_2) & \ldots & \psi_{\alpha_1}(x_N)\\ \psi_{\alpha_2}(x_1) & \psi_{\alpha_2}(x_2) & \ldots & \psi_{\alpha_2}(x_N)\\ \vdots & \ddots & & \\ \psi_{\alpha_N}(x_1) & \psi_{\alpha_N}(x_2) & \ldots & \psi_{\alpha_N}(x_N).\end{bmatrix} \tag{5}$$

It is extremely instructive to write out examples of above N-particle wavefunctions for a few specific cases, e.g., 3 particles with various choices of n_α.

For *interacting* many-body systems, the wavefunction is no longer of above permuted product form, but will still satisfy the same interchange symmetry form, illustrated in Fig.2.

- **Quantum microstates of indistinguishable particles**

  There are two equivalent schemes to label N-particle microstates:

  – Via a set of single particle quantum numbers:

  $$\{\alpha_i\} \equiv (\alpha_1,\alpha_2,\alpha_3,\ldots,\alpha_N),$$

  labeling each of the particles i being in a state α_i. As seen from above N-particle wavefunctions, this is an awkward scheme as it requires symmetrization (bosons) or antisymmetrization (fermions) over particle labels to obtain a probability distribution that is invariant under all particle interchanges.

  The corresponding N-particle energy eigenvalues are given by,

  $$E_{\{\alpha_i\}} = \sum_{i=1}^{N}\varepsilon_{\alpha_i}.$$

– Via a set of occupations $\{n_\alpha\}$ of single particle states α:

$$\{n_\alpha\} \equiv (n_{\alpha_1}, n_{\alpha_2}, n_{\alpha_3}, \ldots),$$

which is very convenient and compact as it automatically does not discriminate, nor even mention which particle is in which state α_i, but only keeps track of the occupations n_α. These are the so-called occupation basis Fock states with each distinct set $\{n_\alpha\}$ labeling a unique many-particle microstate.

$$|n_{\alpha_1}, n_{\alpha_2}, n_{\alpha_3}, \ldots\rangle = |n_{\alpha_1}\rangle|n_{\alpha_2}\rangle|n_{\alpha_3}\rangle \ldots .$$

Thus, correct quantum indistinguishibility weight for quantum many-body states is simply

$$W_Q = 1,$$

per each distinct set of occupations, $\{n_\alpha\}$, with all that matters is the *occupations* n_α, of each of the single particle α states, and *not* which particle i is in which state α.

The corresponding N-particle energy eigenvalues are given by,

$$E_{\{n_\alpha\}} = \sum_\alpha n_\alpha \varepsilon_\alpha.$$

In terms of above labeling we can write down the total number of particles N, as

$$N = \sum_{i=1}^{N} 1 = \sum_\alpha n_\alpha. \tag{6}$$

- **N-particle density matrix**

Now that we have many-body Hamiltonian eigenstates (3),(5), we can construct the canonical ensemble unnormalized N-particle density matrix $\rho^u(x_1, x_2, \ldots, x_N; x'_1, x'_2, \ldots, x'_N; \beta)$ using its general form from Lecture Set 5,

given by

$$\rho^u(\{x_i\},\{x_i'\};\beta) \;=\; \langle\{x_i\}|e^{-\beta\hat{H}}|\{x_i'\}\rangle = \sum_{\{n_\alpha\}} \Psi_{\{n_\alpha\}}(\{x_i\})\Psi^*_{\{n_\alpha\}}(\{x_i'\})e^{-\beta E_{\{n_\alpha\}}}, \quad (7)$$

expressed purely in terms of the Hamiltonian many-body eigenfunctions and eigenvalues, that is a direct analog of single-particle density matrix. Using above (anti)symmetrized product form of eigenstates $\Psi_{\{n_\alpha\}}(\{x_i\})$ we can reduce the N-body density matrix to,

$$\rho^u_{B/F}(x_1,x_2,\ldots,x_N;x_1',x_2',\ldots,x_N') \;=\; \frac{1}{N!}\sum_P (\pm 1)^P \rho^u(x_{P1},x_1')\rho^u(x_{P2},x_2')\ldots\rho^u(x_{PN},x_N'), \quad (8)$$

as a sum over a (anti)symmetrized product of single-particle density matrix $\rho^u(x_i,x_i';\beta) = \langle x_i|e^{-\beta\hat{H}_i}|x_i'\rangle = \sum_\alpha \psi_\alpha(x_i)\psi^*_\alpha(x_i')e^{-\beta\varepsilon_\alpha}$.

- **N-particles in a box example**

  As an example let's consider a noninteracting many-body density matrix for N identical particles in a box, i.e., in a zero potential (except for the box walls).

  single particle properties:

  In the absence of any potential single-particle states are labeled by momentum quantum numbers, $\alpha \to \mathbf{k} = (2\pi/L)\mathbf{n}$ ($\mathbf{n}$ integer-valued vector), corresponding energy eigenvalues $\varepsilon_{\mathbf{k}} = \hbar^2k^2/2m$, and plane-wave eigenstates, $\psi_{\mathbf{k}}(\mathbf{x}) = \frac{1}{V^{1/2}}e^{i\mathbf{k}\cdot\mathbf{x}}$. The corresponding unnormalized 1-particle canonical density matrix we discussed in Lecture Set 5 and derived on the corresponding homework is given by

$$\rho^u(\mathbf{x},\mathbf{x}';\beta) \;=\; \sum_{\mathbf{k}} \psi_{\mathbf{k}}(\mathbf{x})\psi^*_{\mathbf{k}}(\mathbf{x}')e^{-\beta\varepsilon_k} = \frac{1}{V}\sum_{\mathbf{k}} e^{-\beta\hbar^2k^2/2m + i\mathbf{k}\cdot(\mathbf{x}-\mathbf{x}')}, \quad (9)$$

$$\;=\; \left(\frac{m}{2\pi\beta\hbar^2}\right)^{d/2} e^{-\frac{1}{2}m(\mathbf{x}-\mathbf{x}')^2/(\beta\hbar^2)} = \frac{1}{\lambda_T^d}e^{-\pi(\mathbf{x}-\mathbf{x}')^2/\lambda_T^2}, \quad (10)$$

  where $\lambda_T = h/\sqrt{2\pi m k_B T}$ and the prefactor arises from eigenstates' normalization.

  N-particle properties:

The corresponding N-particle eigenstates are given by $\Psi^{\rm B/F}_{\mathbf{k}_1,\ldots,\mathbf{k}_N}(\mathbf{x}_1,\ldots,\mathbf{x}_N)$ from Eqs.(3), (5), and the eigen-energies given by

$$E_{\{n_\mathbf{k}\}} = \sum_i^N \varepsilon_{\mathbf{k}_i} = \sum_\mathbf{k} n_\mathbf{k} \frac{\hbar^2 k^2}{2m}.$$

Utilizing above form of the N-particle eigenstates, general *unnormalized* N-particle density matrix, (8), and the 1-particle density matrix in the absence of a potential (in a large box), simple analysis gives,

$$\rho^u_{B/F}(\mathbf{x}_1,\mathbf{x}_2,\ldots,\mathbf{x}_N;\mathbf{x}'_1,\mathbf{x}'_2,\ldots,\mathbf{x}'_N) \;=\; \frac{1}{N!\lambda_T^{dN}} \sum_P (\pm 1)^P e^{-\pi(\mathbf{x}_{P1}-\mathbf{x}'_1)^2/\lambda_T^2} \ldots e^{-\pi(\mathbf{x}_{PN}-\mathbf{x}'_N)^2/\lambda_T^2}. \tag{11}$$

The diagonal matrix elements (that we use to compute the partition function via $Z = \prod_i^N \int dx_i \rho^u(\mathbf{x}_1,\ldots,\mathbf{x}_N;\mathbf{x}_1,\ldots,\mathbf{x}_N)$) is then given by,

$$\rho^u_{B/F}(\mathbf{x}_1,\ldots,\mathbf{x}_N;\mathbf{x}_1,\ldots,\mathbf{x}_N) \;=\; \frac{1}{N!\lambda_T^{dN}} \left[1 \pm \underbrace{\sum_{i<j} e^{-2\pi(\mathbf{x}_i-\mathbf{x}_j)^2/\lambda_T^2}}_{\text{1 interchange}} + \underbrace{\ldots}_{\text{2 or more interchanges}} \right]. \tag{12}$$

In fact we can now compute the full partition function by integrating over x_i's. Including the lowest order correction (valid on the approach to the degeneracy temperature T_* from above, we obtain,

$$Z_{B/F} \;=\; \int d\mathbf{x}_1 \ldots d\mathbf{x}_N \rho^u_{B/F}(\mathbf{x}_1,\ldots,\mathbf{x}_N;\mathbf{x}_1,\ldots,\mathbf{x}_N), \tag{13}$$

$$\approx\; \int d^N\mathbf{x} \frac{1}{N!\lambda_T^{dN}} \left[1 \pm \sum_{i<j} e^{-2\pi(\mathbf{x}_i-\mathbf{x}_j)^2/\lambda_T^2} \right]. \tag{14}$$

This is a satisfying result with many notable features:

– The dominant first "1" term is exactly the Boltzmann gas result that we obtained a few lectures back crudely treating indistinguishability with the $1/N!$ Gibbs factort, but not fully accounting for the quantum statistics (bosons vs fermions)

of the particles, as we have carefully done above. Upon integrating over $\mathbf{x}_i$s this "1" term then just gives the familiar expression, $Z^{(0)}_{\rm Gibbs} = \frac{V^N}{N!\lambda_T^{dN}}$.

– This fully quantum mechanical calculation confirms the $dpdx/(2\pi\hbar)$ measure for phase-space integration.

– We observe that the correction terms in (12) are strongly subdominant for $\langle r\rangle \gg \lambda_T$, since they involve products of Gaussian factors with $i \neq j$, with the dominant lowest order correction the sum of the double Gaussian terms over all $N(N-1)/2$ $i-j$ pairs. The correction to the classical result are small, i.e., $Z_{B/F} \approx Z^{(0)}_{\rm Gibbs}$ is a good approximation when the typical spacing between particles is much larger than thermal deBroglie wavelength, i.e., $n\lambda_T^d \ll 1$, which corresponds to $T \gg T_*$. This makes sense as in this regime, particles are far apart, their wavefunctions don't overlap, $n_{\mathbf{k}} \ll 1$, particle interchanges and therefore quantum statistics is expected to be insignificant, with Gibbs factor $1/N!$ fully sufficient. In the opposite limit of $n_{\mathbf{k}} \gg 1$, corresponding to $T \ll T_*$, the gas is degenerate, quantum statistics matters, and fermion and bosons N-particle systems exhibit qualitatively distinct phenomenologies as summarized in the first section above and we will explore in detail in the coming sections.

– The factor in the square brackets gives the probability density of finding two particles i and j at the same point for $\mathbf{x}_i = \mathbf{x}_j$. Compared to classical indistinguishable particles, for which it is 1, for bosons it is enhanced to 2 and for fermions it vanishes, 0, consistent with the Pauli's exclusion principle.

– Focussing on 2 particles, the factor in square brackets (proportional to the diagonal component of the 2-particle density matrix) gives the probability density of the two particles at $\mathbf{x}_1$ and $\mathbf{x}_2$,

$$P_{B/F}(\mathbf{x}_1,\mathbf{x}_2) \approx \frac{1}{V^2}\left[1 \pm e^{-2\pi(\mathbf{x}_1-\mathbf{x}_2)^2/\lambda_T^2}\right], \tag{15}$$

$$\equiv \frac{1}{V^2} e^{-U_{\rm q.stat}(|\mathbf{x}_1-\mathbf{x}_2|)/k_BT}, \tag{16}$$

where we wrote $P_{B/F}(\mathbf{x}_1.xv_2)$ as a Boltzmann-Gibbs weight, so that we can interpret this quantum statistical "interaction" in terms of an effective interaction potential $U_{\rm q.stat}(|\mathbf{x}_1-\mathbf{x}_2|)$ associated with the effective quantum statistical inter-

action between particles, given by

$$U_{\rm q.stat}(|\mathbf{x}|) \;=\; -k_BT\ln\left[1\pm e^{-2\pi|\mathbf{x}|^2/\lambda_T^2}\right]\approx \mp k_BTe^{-2\pi|\mathbf{x}|^2/\lambda_T^2}, \tag{17}$$

which is attractive for bosons and repulsive for fermions. Notice that it is proportional to k_BT, which when multipled by β in Gibbs-Boltzmann weight, (16) gives probability distribution that is temperature independent, underscoring its purely quantum statistical nature.

– Using the quantum canonical partition function (14), we can compute the free energy and all other thermodynamics. In particular, a straightforward calculation of the pressure in 3d gives,

$$P_{B/F} \;\approx\; k_BT\frac{N}{V}\left[1\mp\frac{(N-1)\lambda_T^3}{2^{5/2}V}\right]\approx k_BTn\left[1\mp 2^{-5/2}\;n\lambda_T^3\right]. \tag{18}$$

This result is a first-order correction to the ideal gas $P=k_BTn$ equation of state in powers of $n\lambda_T^3\ll 1$ due to quantum statistical interaction, and of course breaks down as the degeneracy regime is approached at T_*.

III. N-PARTICLE QUANTUM THERMODYNAMICS

Having established above the fundamentals of quantum many-body statistical mechanics, we can now apply them to calculate the thermodynamics of variety of important systems such as Bose and Fermi gases in various physical realizations. These will include Bose-Einstein condensation of atoms, black-body radiation of photons, and phonons in solids, of electrons in metals, exhibiting Pauli paramagnetism, and of neutrons in neutron stars.

We first recall that the microstates of indistinguishable quantum particles is characterized by the occupation numbers $\{n_\alpha\}$ of single-particle states α. For bosons, occupation numbers are unlimited, taking on integers, $n_\alpha = 0,1,2,3,\ldots$. In striking contrast, for fermions, the Pauli principle limits the occupation numbers to $n_\alpha = 0,1$ for each single-particle state α, i.e., it can either be empty or filled by a single fermion.

We can now straighforwardly compute the grandcanonical partition function, given by

$$\mathcal{Z}_{\mathrm{B/F}} \;=\; \sum_{\{n_\alpha\}} e^{-\Big(E[\{n_\alpha\}]-\mu N[\{n_\alpha\}]\Big)/k_BT} = \sum_{\{n_\alpha\}} e^{-\sum_\alpha n_\alpha(\varepsilon_\alpha-\mu)/k_BT} = \prod_\alpha \left[1\mp e^{-(\varepsilon_\alpha-\mu)/k_BT}\right]^{\mp 1}, \tag{19}$$

which then immediately gives the correspoinding grandcanonical free energy, $\mathcal{F} = -k_BT\ln\mathcal{Z}$,

$$\mathcal{F}_{\mathrm{B/F}} \;=\; \pm k_BT\sum_\alpha \ln\left[1\mp e^{-(\varepsilon_\alpha-\mu)/k_BT}\right], \tag{20}$$

and the rest of thermodynamics obtained via appropriate derivative with respect to T, μ, or V. In particular, as advertized in the summary of the introduction, the average number of particles is given by $N = -\partial\mathcal{F}/\partial\mu|_{T,V} = \sum_\alpha n_\alpha^{\mathrm{B/F}}$, where $n_\alpha^{\mathrm{B/F}}$ is the bosonic/fermionic occupation of the single-particle state α,

$$n_\alpha^{\mathrm{B/F}} \;=\; \frac{1}{e^{(\varepsilon_\alpha-\mu)/k_BT}\mp 1}. \tag{21}$$

We note that above general results are all controlled by the single particle spectrum, ε_α, that depends on the single particle potential $U(r)$ that the noninteracting bosons are moving in. Some relevant familiar examples are infinite square-well potential, vanishing potential with periodic boundary conditions, or e.g., a harmonic trap, $U(r) = \frac{1}{2}m\omega_{\mathrm{trap}}^2 r^2$, as utilized in atomic gas experiments. We next focus on a specific example of a potential-free atoms, or more precisely atoms in a box with periodic boundary conditions.

A. Noninteracting atomic Bose gas and BEC

We now want to calculate the thermodynamics of a noninteracting Bose gas as for example found in dilute degenerate atomic Bose gases (laser and evaporatively) cooled in JILA and around the world. It is crucial to note that here we are dealing with a system of *conserved* bosons, as to be contrasted to applications of photons and phonons excitations treated in the subsequent sections.

1. High-temperature thermodynamics

To fix the number of bosonic atoms to be N it is convenient to work in the grand-canonical formulation of quantum statistical mechanics. We tune the chemical potential μ such that the expectation value of the atom number is given by the experimentally prescribed atom number $\overline{N}$,

$$\begin{aligned}
\overline{N} &= \sum_{\mathbf{k}} n^{\mathrm{BE}}(\epsilon_{\mathbf{k}}) = \sum_{\mathbf{k}} \frac{1}{e^{\beta(\epsilon_{\mathbf{k}}-\mu)}-1}, && (22)\\
&= L^d \int \frac{d^d k}{(2\pi)^d} \frac{1}{e^{\beta(\epsilon_{\mathbf{k}}-\mu)}-1} = V\frac{C_d}{2}\left(\frac{2m}{\hbar^2}\right)^{d/2} \int_0^\infty d\epsilon \frac{\epsilon^{d/2-1}}{e^{\beta(\epsilon-\mu)}-1}, && (23)\\
n &= \frac{1}{\lambda_T^d} g_{d/2}(z), && (24)
\end{aligned}$$

where $\epsilon_{\mathbf{k}} = \hbar^2 k^2/2m$ is the familiar single-particle energy eigenvalues, and in going to the next-to-last line we made (what will turn out to be) a crucial thermodynamic limit approximation, replacing sum over $\mathbf{k}$ by an integral, and then followed by the integral over the single-particle energies ϵ (rather than states $\mathbf{k}$) after doing the angular integration. Above, $C_d = S_d/(2\pi)^d = 1/(2^{d-1}\pi^{d/2}\Gamma(d/2))$, where $S_d = 2\pi^{d/2}/\Gamma(d/2)$ is a surface area of a d-dimensional unit hypersphere. In the last line we scaled out $k_B T$ and thereby expressed the average density $n = N/V$ in a compact and dimensionally appealing form as the thermal deBroglie density, fugacity $z = e^{\mu/k_B T}$ and introduced a dimensionless function of z,

$$g_\nu(z) = \frac{1}{\Gamma(\nu)} \int_0^\infty \frac{x^{\nu-1}}{e^x z^{-1} - 1} = \sum_n b_n^{(\nu)} z^n = z + \frac{z^2}{2^\nu} + \frac{z^3}{3^\nu} + \ldots . \qquad (25)$$

All together, this gives us an implicit relation between N and the chemical potential, μ (or fugacity z), $n\lambda_T^d = g_{d/2}(z)$, which when inverted gives us $\mu(N,T)$, allowing us to express any thermodynamic quantity in terms of density n and temperature, T. Namely,

Utilizing (19) and (20) then also gives us the grand-canonical partition function and the corresponding free energy and pressure,

$$\begin{aligned}
\mathcal{Z}_{\mathrm{B}} &= \prod_{\mathbf{k}} \frac{1}{1-e^{-(\epsilon_{\mathbf{k}}-\mu)/k_B T}}, && (26)\\
\mathcal{F}_{\mathrm{B}} &= k_B T \sum_{\mathbf{k}} \ln\left[1 - e^{-(\epsilon_{\mathbf{k}}-\mu)/k_B T}\right], && (27)
\end{aligned}$$

from which all of the thermodynamics can be extracted as a function of μ, T, V, or equivalently (having used (24) to eliminate $\mu(T, V, N)$) as a function of N, T, V. The key quantity is the equation of state, namely the pressure $P(T, V, N)$, directly obtained from $q = \ln \mathcal{Z}$.

At high temperature the gas should behave as a classical Boltzmann gas with a negative chemical potential. Indeed in that regime we can ignore 1 relative to the exponential and straightforwardly perform the integration. Solving for the chemical potential in terms of the density $n = N/V$ and temperature we obtaining the classical Boltzmann result:

$$\mu(T, n) = k_B T \ln(n\lambda_T^d) = -k_B T \frac{d}{2} \ln(c_d T/T_*), \quad \text{valid for } T \gg T_* \tag{28}$$

where

$$\lambda_T = \left(\frac{2\pi\hbar^2}{m k_B T} \right)^{1/2}$$

is the familiar thermal deBroglie wavelength and we deduced the crossover degeneracy temperature scale

$$k_B T_* = \frac{\hbar^2 n^{2/d}}{2m},$$

above which this classical result is valid and the quantum Bose gas "forgets" its statistics and behaves like a Boltzmann gas.

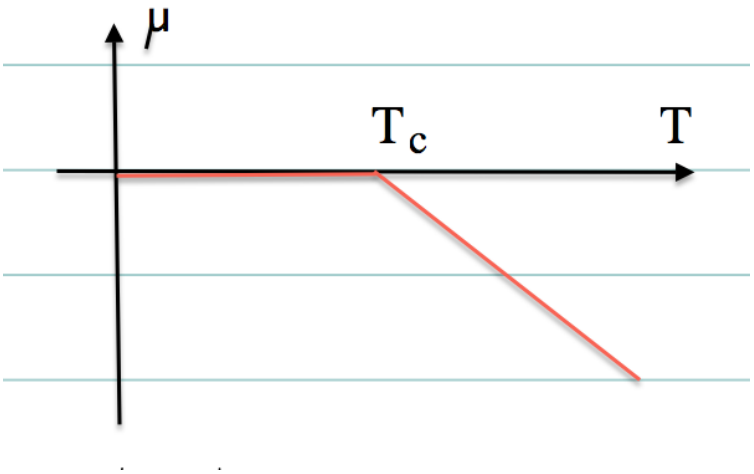

FIG. 3: Chemical potential in a noninteracting Bose gas as a function of temperature near the transition to Bose-Einstein condensation at temperature T_c.

Following the number equation analysis, (24) by going to the thermodynamic limit $L \to \infty$, from (27) and $E = -\partial_\beta \ln \mathcal{Z}_B|_{z,V}$, we obtain the equation of state, P and internal energy

density E/V,

$$P = \frac{k_B T}{\lambda_T^d} g_{d/2+1}(z), \tag{29}$$

$$E/V = \frac{d}{2} \frac{k_B T}{\lambda_T^d} g_{d/2+1}(z), \tag{30}$$

giving pressure-energy density relation,

$$P = \frac{2}{d} \frac{E}{V}.$$

Eliminating z in favor of $n\lambda_T^d$, from above we also obtain the "virial expansion" for the equation of state, at high temperature for $T \gg T_*$ (when $n\lambda_T^d \gg 1$),

$$\frac{PV}{Nk_B T} = \frac{g_{d/2+1}(z)}{g_{d/2}(z)} = \sum_{\ell=1}^{\infty} a_\ell (n\lambda_T^d)^{\ell-1}, \tag{31}$$

where a_ℓ are virial coefficients, that measure deviation from the ideal gas equation of state. This, together with (30) is to be contrasted with the ideal gas law and the equipartion, both of which are violated at low T as the degeneracy temperature T_* is approached. Although these are violated as the gas approaches degeneracy, interestingly, the $P - E$ relation is identical to that of an ideal gas. Returning to our earlier result for pressure, (18), we see that $a_1 = 1$ (ideal gas law), $a_2 = -2^{-5/2}$, measuring lowest order quantum statistics deviation from the ideal gas law.

Similarly, the heat capacity can be straightforwardly computed above T_* in a virial expansion, giving,

$$C_V = \frac{d}{2} N k_B \left[1 + c_1 (n\lambda_T^d)^1 + c_2 (n\lambda_T^d)^2 + \ldots\right]. \tag{32}$$

2. Low-temperature thermodynamics and BEC

We now consider what the behavior of above thermodynamic quantities as we lower temperature toward and below T_*. First, let's focus on the number equation, (24). As we noted above, (28), for $T \gg T_*$, $\mu < 0$ and correspondingly $z \ll 1$ in the high temperature Boltzmann limit. We observe that as T is lowered, chemical potential can be increased (from

negative value toward zero), as illustrated in Figs.(3) and (4), to continue to satisfy the N condition, (24). Now, the crucial question is about the behavior of $\mu(T,N)$ as $T \to T_*$. In the discrete sum over $\mathbf{k}$ description

$$N = \frac{1}{e^{(0-\mu)/k_BT}-1} + \frac{1}{e^{(\epsilon_1-\mu)/k_BT}-1} + \dots \tag{33}$$

(22) clearly can always be satisfied, but adjusting, i.e., with reduced T raising μ toward zero, because the first zero-energy term can be made arbitrarily large no matter how large N is and how low T is. Thus, down to zero temperature there is a *smooth* analytic evolution of $\mu(T,N)$, and thus *no phase transition* in a box of finite size L.

For $d \leq 2$, the integral in (23) and therefore $g_{d/2}(z \to 1)$ diverges with vanishing μ (note that e.g., for $\nu = 1$, $g_1(z) = -\ln(1-z)$ and $g_1(z \to 1) \to \zeta(1) = \infty$) and thus this number N constraint can be satisfied down to zero temperature by simply adjusting the negative chemical potential, $\mu(T,N)$ closer to zero to accommodate lower T and larger N, even in the thermodynamic limit. This is manifestation of the famous Hohenberg-Mermin-Wagner-Coleman theorem, that (under certain pretty generic conditions) forbids spontaneous breaking of continuous symmetries and the associated condensate in $d \leq 2$.[7]

However, in thermodynamic limit $L \to \infty$, replacing a sum over discrete $\mathbf{k}_n$ by an integral over $\mathbf{k}$ or over ϵ, an apparent "problem" appears in $d > 2$ (in particular for the physical case of interest, $d = 3$) in (23). Namely, the equation cannot be satisfied for sufficiently large N or sufficiently low T as the integral saturates to a finite value. This happens because the "area" under $n^{\rm BE}(\epsilon)$ is finite even at $\mu = 0$ for $d > 2$. Why can't we simply allow μ to be positive to continue satisfying the number equation? The saturations is a consequence of a density of states, the integral does an inadequate job of accounting for the low k states that at low $T < T_c$ are macroscopically occupied (see below). The high power of k (k^{d-1}) or ϵ ($\epsilon^{d/2-1}$) in the numerator make the integral convergent at low momenta and energies that vanishes more strongly with increased dimension, $d > 2$. Namely, as illustrated in Fig.4, for $d > 2$ the integral in (23) saturates at a finite value even for $\mu = 0$, i.e., $z = 1$, and the continuum equation reduces to,

$$n\lambda_{T_c}^d = g_{d/2}(1) = \zeta(d/2),$$

where $\zeta(x)$ is the Riemann-zeta function, which for $\xi(3/2) \approx 2.61$ ($d = 3$), but diverges for $x \leq 1$, corresponding to $d \leq 2$. Above equation implicitly defines a "critical temperature" T_c, given by,

$$k_B T_c = \frac{4\pi}{\zeta(d/2)^{2/d}} \frac{\hbar^2 n^{2/d}}{2m} = \frac{4\pi}{\zeta(d/2)^{2/d}} k_B T_*, \quad \text{valid for } d > 2, \tag{34}$$

as the lowest temperature above which all N particles can be accommodated in the Bose-Einstein distribution and thereby can satisfy the thermodynamic limit of the number equation, (23) or (24). We note that T_c increases with reduced atom mass and increased density, enhancing the role of quantum fluctuations. As we will see below, this is the Bose-Einstein condensation temperature, below which a macroscopic number of bosonic atoms begin to occupy the single-particle ground state. In 3d the critical temperature is given by $T_c = 6.625 T_*$, of order of the degeneracy temperature T_*.

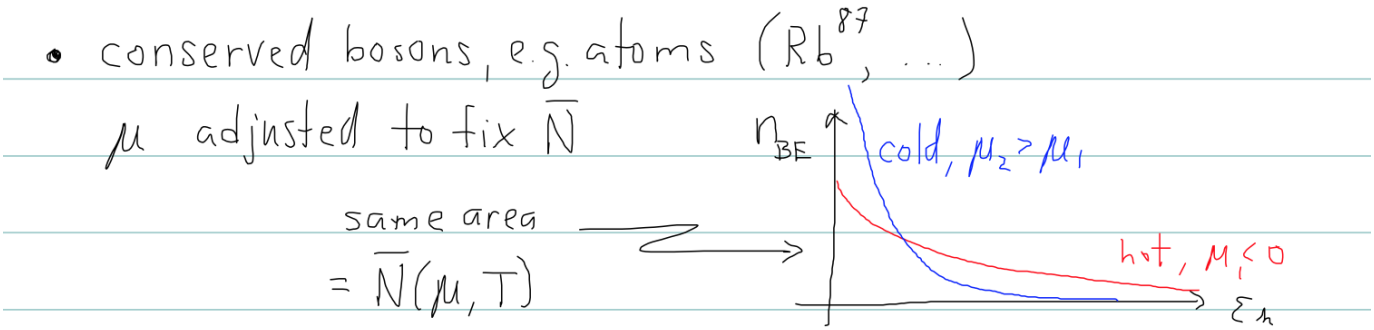

FIG. 4: A sketch of the Bose-Einstein momentum distribution function as a function of k as T is reduced toward T_c from above.

How do we fix this deficiency of the thermodynamic limit description? The clew appears in Eq.(33). To account for the discreteness of low energy states, as illustrated in Fig.(5), we separate out the single particle ground state $\mathbf{k} = 0$ and simply describe its occupation by $N_0(T) = n_0 V$, the Bose-Einstein condensate (BEC),

$$\begin{aligned} N &= \frac{1}{e^{-\mu/k_B T} - 1} + L^d \int \frac{d^d k}{(2\pi)^d} \frac{1}{e^{\beta(\epsilon_{\mathbf{k}} - \mu)} - 1}, \\ &= N_0(T) + L^d \int \frac{d^d k}{(2\pi)^d} \frac{1}{e^{\beta(\epsilon_{\mathbf{k}} - \mu)} - 1}, \qquad (35) \\ &= N_0(T) + \frac{V}{\lambda_T^d} g_{d/2}(z), \qquad (36) \end{aligned}$$

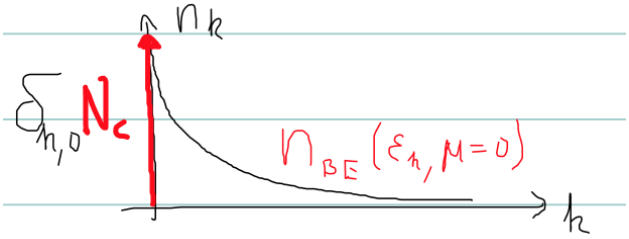

FIG. 5: A sketch of the Bose-Einstein momentum distribution function $n_{\mathbf{k}}^{\rm BE}$ as a function of $\mathbf{k}$ for $T < T_c$, illustrating the thermal finite $\mathbf{k}$ and the condensate $\mathbf{k} = 0$ component.

that accommodates all the extra atoms unable to "fit" into the nonzero $\mathbf{k}$ states counted by the integral of the Bose-Einstein distribution in Eq. (23). For $T > T_c$, $N_0 = 0$, i.e., no BEC, and for $T < T_c$, $\mu = 0$ and BEC appears, $N_0(T < T_c) > 0$, with $n_0(T < T_c) = N_0/V$ growing according to,

$$n_0(T) = n\left[1 - \left(\frac{T}{T_c}\right)^{d/2}\right], \quad \text{for } T < T_c, \tag{37}$$

$$\sim |T_c - T|^{2\beta}, \tag{38}$$

as illustrated in Fig.(6). The last equality applies in the vacinity of T_c, with the mean-field critical exponent $\beta = 1/2$, characterizing the transition for noninteracting bosons.

The number density of finite-temperature excitations is then given by the complement of n_0, i.e., $n - n_0(T)$,

$$n_{\rm exc}(T) = n\left(\frac{T}{T_c}\right)^{d/2}.$$

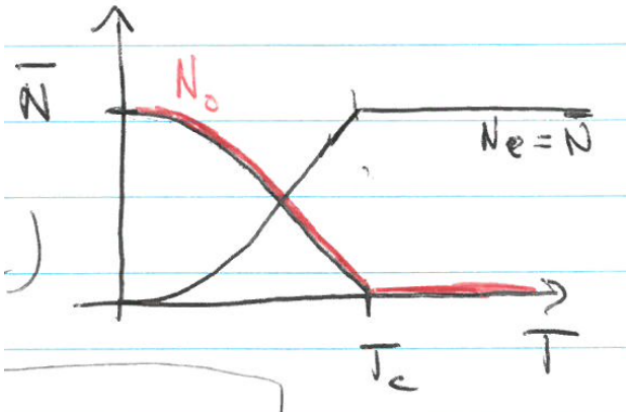

FIG. 6: A sketch of the condensate fraction $N_0(T)$ and its complement, $N_e(T)$, the number of excitations at finite T.

We thus discovered the existence of a finite-temperature phase transition in an noninteracting Bose gas, between thermal Boltzmann gase and Bose-Einstein condensed phases. From above we also find that for noninteracting bosons, in the thermodynamic limit, the chemical potential vanishes below T_c, i.e., $\mu(T < T_c) = 0$, as illustrated in Fig.(3). A careful analysis of (35) shows that in 3d,

$$\mu(T) = -k_B T \frac{(n\lambda_T^3)^2}{4\pi} \left[\left(\frac{T}{T_c} \right)^{3/2} - 1 \right]^2 \sim -(T - T_c)^2, \quad \text{for } T > T_c.$$

At low temperature $T \ll T_c$, the internal energy $E(T)$ and heat capacity $C_V(T)$ are straightforwardly computed by noting that $\mu = 0$ which allows one to simply scale out T out of the integrals in (30). This then gives,

$$E(T) \sim T^{d/2+1}, \quad T \ll T_c, \tag{39}$$

$$C_V(T) \sim T^{d/2}, \quad T \ll T_c. \tag{40}$$

We note:

- The excitations are gapless, appearing as power-law in T at arbitrary low T, illustrated in Fig.(7). This is to be contrasted with gapped systems, where $C_V(T) \sim e^{-\Delta/k_B T}$ is strongly (exponentially) suppressed at low $T < \Delta/k_B$.

- No equipartition for this quantum limit

- Ground state condensate does not contribute to the energy nor heat capacity, since it sits at a vanishing energy. Thus, $E(T), C_V(T)$ are independent of N.

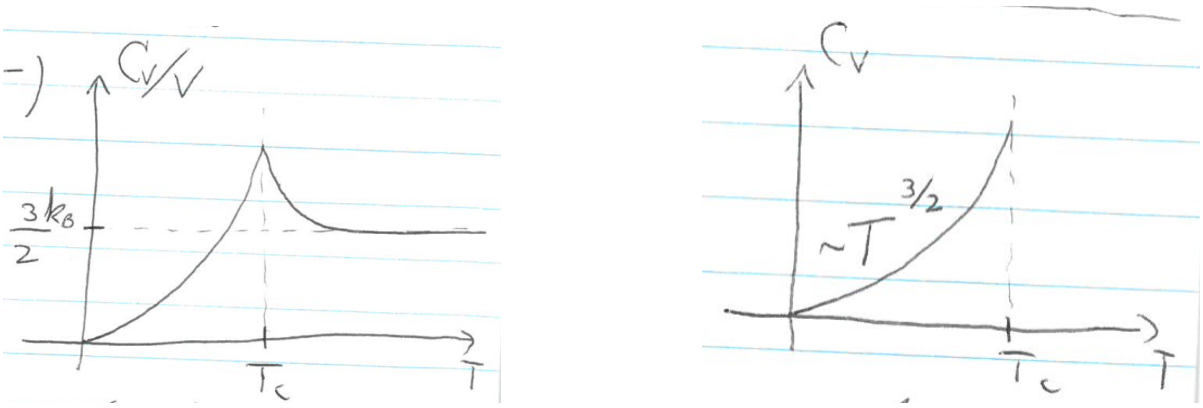

FIG. 7: Heat capacity as a functon of temperature of a 3d Bose condensate and its zoom-in at low temperatures.

At $T = 0$ the BEC is as simple as they come, with all N atoms occupying the lowest single-particle ground state, $\mathbf{k} = 0$, $N_0 = N$, described by a many-body state,

$$|\Psi_0\rangle = \left(a^\dagger_{\mathbf{k}=0}\right)^N |0\rangle, \tag{41}$$

that corresponds to a wavefunction that is a product of the single-particle ground state wavefunction $\psi_0(\mathbf{r})$ occupied by each atom,

$$\Psi_0(\mathbf{r}_1, \mathbf{r}_2, \ldots, \mathbf{r}_N) = \prod_{i=1}^{N} \psi_0(\mathbf{r}_i) = \frac{1}{V^{N/2}}.$$

The last equality corresponds to the case of a box trap that we worked out above. In a more relatistic harmonic isotropic trap, relevant to AMO experiments, instead the single particle ground state is the familiar Gaussian, $\psi_0(\mathbf{r}) \sim e^{-\frac{1}{2}r^2/r_0^2}$, with $r_0^2 = \sqrt{\hbar/(m\omega_{\rm trap})}$ the trap's quantum oscillator length.

We note that without interactions the condensate $n_0(T)$ grows from zero, approaching total atomic density n at $T = 0$. This last property is not generic and will not survive inclusion of atomic interactions. These and all other properties of this noninteracting system can and have been extensively explored theoretically and experimentally in the last 25 years in degenerate atomic gases (see e.g.,[1, 16]). The phenomenology of interacting bosonic liquids

is far more challenging to treat theoretically, but experimentally dates back to extensive exploration of He^4, that resembles some but not all features of the BEC described above.

B. Black-body radiation of a photon gas

We now turn to the study of a very different type of bosons, namely bosonic excitations of electromagnetic field, i.e., photons. The crucial difference from bosonic atomcs is the nonconservation of these bosonic excitations. Thus, the chemical potential is not necessary to fix their number N, which amounts to working at $\mu = 0$, without the number equation (22). This therefore precluding BEC, though some experimental systems can be arranged to mimic nonequilibrium version of a BEC even in photons, e.g., laser or other steadily driven/pumped systems.

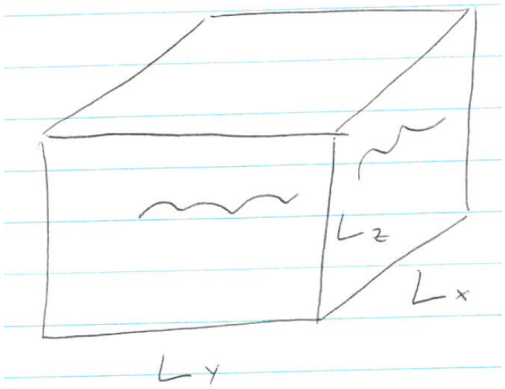

FIG. 8: Black body radiation of photons in a cavity

We thus consider a gas of photons in a box, again for convenience taking periodic boundary conditions in all directions, though this is not essential. Physically and in practice this pretty much corresponds photons going off any glowing body at temperature T, like e.g., the Sun, the Earth, microwave background radiation, a hot stove, etc. However, more precisely we would like the photons to remain confined to the cavity (box) and in equilibrium at temperature T, rather than a nonequilibrium situation of an open system, where photons are escaping.

Other than the nonconserved number of photons, with $\mu = 0$, the description of a gas of photons parallels that of atoms in the previous section. One other notable difference is that photon's single-particle dispersion, being a mass zero, ultra-relativisitic particle, is *linear*

(rather than quadratic) in k, given by

$$\varepsilon_{\mathbf{k}} = \hbar\omega_{\mathbf{k}} = \hbar c|\mathbf{k}|,$$

labelled by the single-particle quantum numbers $\mathbf{k}$, the EM modes of the cavity.

Equivalently, in a formulation due to Planck (1900), that predates Bose and Einstein (1924), we can instead think of quantized modes of a EM cavity waves, labelled by discete quantum numbers $\mathbf{k}$, i.e., quantum harmonic oscillators at each mode $\mathbf{k}$. Utilizing our knowledge of thermodynamics of independent quantum oscillators we immediately obtain in 3d,

$$\begin{aligned}
\mathcal{Z} &= \prod_{\mathbf{k},\alpha=(1,2)} Z_{\mathbf{k},\alpha} = \prod_{\mathbf{k}} \left[\sum_{n_{\mathbf{k}}} e^{-\beta\hbar\omega_k n_{\mathbf{k}}}\right]^2 = \prod_{\mathbf{k}} \left[\frac{1}{1-e^{-\beta\hbar\omega_k}}\right]^2, \qquad (42)\\
\frac{E}{V} &= -\frac{1}{V}\frac{\partial \ln \mathcal{Z}}{\partial\beta} = \frac{1}{V}\sum_{\mathbf{k}} \frac{2\hbar\omega_k}{e^{\beta\hbar\omega_k}-1},\\
&= \int \frac{d^3k}{(2\pi)^3}\frac{2\hbar ck}{e^{\beta\hbar ck}-1} \equiv \int d\omega u(\omega), \qquad (43)\\
&= \frac{\pi^2}{15(\hbar c)^3}(k_B T)^4 = \frac{4}{c}\sigma T^4, \qquad (44)
\end{aligned}$$

where the factor of 2 came from two independent transverse polarizations of EM modes per $\mathbf{k}$ (that we took to be degenerate), we went to a continuum limit ($L \to \infty$), recovered the famous T^4 Stefan-Boltzmann law (1879) and introduced a spectral density $u(\omega)$ given by,

$$u(\omega) = \frac{\hbar}{\pi^2 c^3}\frac{\omega^3}{e^{\beta\hbar\omega}-1} \qquad (45)$$

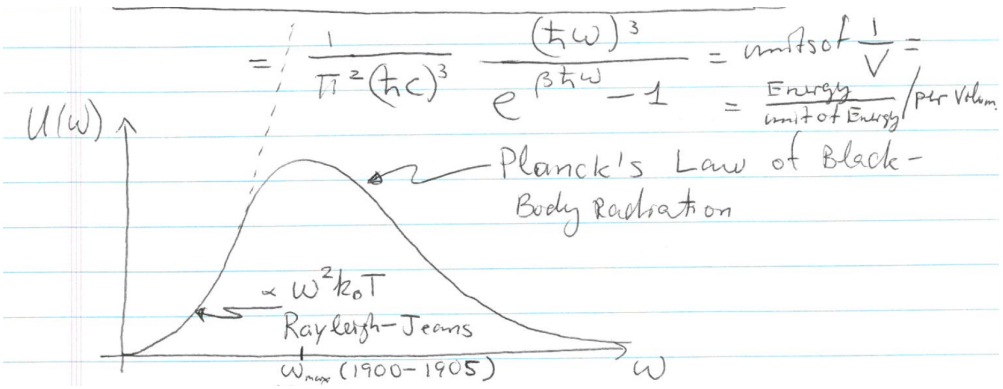

FIG. 9: Black body thermodynamics, Stefan-Boltzmann law (1879)and the corresponding Planck's spectral density, and its classical Rayleigh-Jeans limit.

Observations:

- Units of $u(\omega)$ are (energy/per unit of energy) per unit of volume. Sometimes, one is interested in "radiance", L which is the corresponding energy flux per unit of solid angle (the observable of the radiation flux leaking out of the box), with units of energy per unit of time/per length squared, obtained by $L = (c/4)E/V$.

- The $E \sim T^4$ result can be qualitatively understood as the total energy of the modes that obey equipartition, i.e., those for which $\hbar\omega_k \ll k_B T$, corresponding to the maximum $k_T = k_B T/(\hbar c)$. Modes at larger frequencies ($k \gg k_T$) are gapped out and therefore exponentially suppressed with $e^{-\hbar\omega_k/k_B T}$. Thus, the total energy per unit of volume is given by $k_B T$ per mode times the number of modes $N(T) = 2\int_0^{k_T=\frac{k_B T}{\hbar c}} \frac{d^3k}{(2\pi)^3} \sim k_T^3 \sim [k_B T/(\hbar c)]^3$, up to a dimensionless prefactor giving the result $[k_B T/(\hbar c)]^3 k_B T$ in (44).

- Computation of the Stefan-Boltmann factor just involves change of variables with the numerical prefactor $\gamma = \int_0^\infty \frac{dx x^3}{e^x - 1} = \zeta(4)\Gamma(4) = \pi^4/15$, that can be obtained by a Taylor expansion in e^{-x}. The Stefan-Boltzmann constant $\sigma = \frac{\pi^2 k_B^4}{60\hbar^3 c^2} = 5.67 \times 10^{-8}$ Watt/m^2/K^4.

- At low frequencies ω (energies $\hbar\omega \ll k_B T$), the spectral density reduces to $u_{\rm cl}(\omega) = \frac{\omega^2}{\pi^2 c^3} k_B T$, that, as expected corresponds to that of the *classical* harmonic oscillator that obeys equipartition. This Rayleigh-Jeans law leads to the famous "ultraviolet catastrophy" of a divergent black-body total energy, that was instrumental to the launched of quantum revolution.

- Computing the photon pressure from $PV/k_B T = \ln \mathcal{Z}$, gives a very similar relation to E above, with the photon equation of state,

$$PV = \frac{1}{3}E,$$

as expected from ultra-relativistic dispersion on general grounds (see earlier lectures and homework) and to be contrasted with the 3d nonrelativistic Boltzmann gas $PV = \frac{2}{3}E$..

- The photon entropy and heat capacity is also straightforwardly obtained, given by $S = \frac{4}{3}E/T$, and $C_V \sim T^3$ ($\sim T^d$ in d dimensions).

C. Phonons in a solid

We now turn to another example of bosonic excitations, namely the so-called quanta of normal mode vibrational excitations in coupled ions in Debye solid (1912). The ions in a solid are interacting with Coulomb interactions, potentially screened by electrons. However, at low energies (temperatures), the solid is stable with inter-ion potential well-approximated by a harmonic form, depicted as linear springs in Fig.(10). The resulting system is thus that of linearly coupled linear harmonic oscillators, with Hamiltonian,

$$H = \sum_{\mathbf{x}_n} \frac{\mathbf{p}_{\mathbf{x}_n}^2}{2m} + \sum_{\mathbf{x}_n+\vec{\delta}} \frac{1}{2}\kappa(\mathbf{u}_{\mathbf{x}_n} - \mathbf{u}_{\mathbf{x}_n+\vec{\delta}})^2 \tag{46}$$

with $\vec{n}$ spanning the lattice and $\vec{\delta}$ nearest neighbors of site $\vec{n}$.

We decouple these oscillators into normal modes,

$$\mathbf{u}(\mathbf{x}_n, t) = \sum_{\mathbf{k},\alpha=(1,2,3)} \mathbf{u}_{\mathbf{k},\alpha} e^{i(\mathbf{k}\cdot\mathbf{x}_n - \omega_{k,\alpha}t)}, \tag{47}$$

where α labels 3 polarizations per normal mode $\mathbf{k}$ in 3d. Notice the subtle difference from photons, that because they are gauge bosons only have 2 transverse polarizations per $\mathbf{k}$ in 3d.

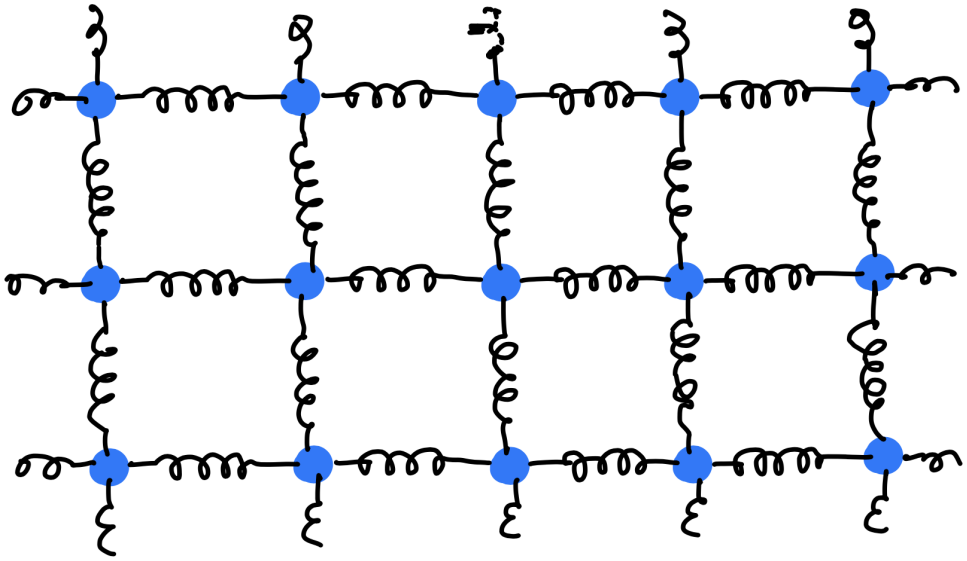

FIG. 10: A crystal of ions, modeled as N coupled harmonic oscillators, the so-called Debye solid (1912). The corresponding quanta of normal mode excitations are phonons.

In terms of normal modes $\mathbf{u}_{\mathbf{k},\alpha}$, the Hamitonian (46) decouples into independent harmonic oscillators, 3 for each $\mathbf{k}$. Treating these as quantum oscillators quantizes the modes of vibration as for any set of independent quantum oscillators. As discussed multiple times, the microstates are the labelled by the set of occupation numbers $\{n_{\mathbf{k},\alpha}\}$, with the corresponding microstate energy eigenvalues given by

$$E_{\{n_{\mathbf{k},\alpha}\}} = \sum_{\mathbf{k},\alpha} \hbar\omega_{k,\alpha} n_{\mathbf{k},\alpha},$$

where we have omitted the zero-point energy constant. Standard analysis (as e.g., given for photons, above, (44), and really for any independent quantum harmonic oscillators) gives

the thermodynamics and in particular the total energy density,

$$\frac{E}{V} = \frac{1}{V}\sum_{\mathbf{k}\in\text{B.Z.},\alpha}\frac{\hbar\omega_{k,\alpha}}{e^{\beta\hbar\omega_{k,\alpha}}-1} = \sum_{\alpha}^{3}\int_{\text{BZ}}\frac{d^3k}{(2\pi)^3}\frac{\hbar\omega_{k,\alpha}}{e^{\beta\hbar\omega_{k,\alpha}}-1}, \tag{48}$$

$$= \frac{1}{V}\int d\omega g(\omega)\frac{\hbar\omega}{e^{\beta\hbar\omega}-1} \equiv \int d\omega u(\omega), \tag{49}$$

$$C_V = \frac{\partial E}{\partial T} = k_B\sum_{\mathbf{k}\in\text{B.Z.},\alpha}\frac{(\beta\hbar\omega_{k,\alpha})^2 e^{\beta\hbar\omega_{k,\alpha}}}{(e^{\beta\hbar\omega_{k,\alpha}}-1)^2}, \tag{50}$$

$$= k_B\int d\omega g(\omega)\frac{(\hbar\omega/k_BT)^2 e^{\hbar\omega/k_BT}}{(e^{\hbar\omega/k_BT}-1)^2} \tag{51}$$

where $g(\omega)$ is the density of states (think of multiplicity that counts number of states at energy $\hbar\omega$), formally defined by,

$$g(\omega) = \sum_{\mathbf{k}\in\text{B.Z.},\alpha}\delta(\omega-\omega_{k,\alpha}) \tag{52}$$

The expression (51) parallels that for photons (44) with few important differences:

- The spectrum $\hbar\omega_{k,\alpha}$ strongly depends on the type of a lattice and because the crystal is generically not isotropic depends on the polarization α.

- Because the model is that of a discrete set of atoms with $3N$ distortions $\mathbf{u}_{\tilde{\mathbf{n}}}$ the total number of normal modes must also be $3N$ in 3d (the number of normal modes must equal to the total number of the original degrees of freedom of N atoms with 3d displacements, since former are just linear combination of the latter), the range of $\mathbf{k}$ is limited to the so-called Brillouin Zone. This is nothing more than what you find in 1d Fourier series (as opposed to Fourier integrals), where the integral is limited to a finite region corresponding to the period of the system. Physically this arises because there is no meaning to excitation at $\mathbf{k}$ outside of the BZ (roughly $k_{\max} = 2\pi/a$, where a is lattice spacing), since it corresponds to wavelengths that are smaller than interion separation a, which is just empty space, with such distortion having no physical meaning. This is strikingly different than infinite number of $\mathbf{k}$ modes of an EM wave excitations (photons) since space these waves live in is continuous, labeled by $\mathbf{x}$ rather than by a discrete coordinate $\vec{n}$.

- The fully detailed model of these modes depends strongly on the type of crystal con-

sidered and is beyond the scope of our analysis here.

All the information about the type of phonons is packaged into the density of states, $g(\omega)$, that satisfies

$$\int_0^\infty d\omega g(\omega) = \sum_{\mathbf{k}\in \text{B.Z.},\alpha} 1 = 3N, \tag{53}$$

counting the total number of normal modes. All phonons types fall into two classes of phonon model, the so-called Einstein model (1907) and the Debye model (1912), that we study below.

Phonon models

We now consider two simplified models of phonons that qualitatively capture all common physical situations, corresponding to optical (Einstein's gapped) and acoustic (Debye's gapless) phonons. These are determined by the $\omega_{k,\alpha}$ or equivalently by the density of states $g(\omega)$.

1. Optical Einstein phonons

Optical phonons appear in ionic solids and by looking at lattices with more than one atom per unit cell. Their key property is that they are gapped, as illustrated in Fig.(11).

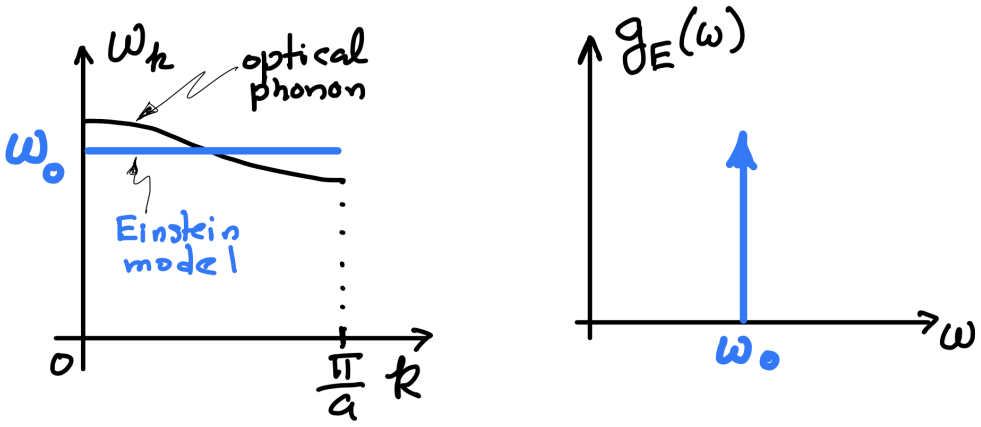

FIG. 11: (a) A dispersion of an optical phonon, modeled by a nondispersive Einstein phonon with $\omega_{k,\alpha} = \omega_0$. (b) The density of states for Einstein phonons, with all $3N$ degenerate modes appearing at a single frequency ω_0, modelled by a δ-function, corresponding to (a).. A simplest lattice model of Einstein phonon is that of decoupled ions.

For a simplified model of such optical phonons we replace the gapped $\omega_{k,\alpha}$ with narrow bandwidth dispersion by simply $\omega_{k,\alpha} \approx \omega_0$ nondispersive Einstein phonon with zero bandwidth, and corresponding δ-function density of states,

$$g_E(\omega) = 3N\delta(\omega - \omega_0),$$

with the amplitude fixed by the total number of $3N$ modes, as illustrated in Fig.(**??**).

Corresponding to this Einstein model we then obtain,

$$C_V \;=\; 3Nk_B \frac{(\hbar\omega_0/k_BT)^2 e^{\hbar\omega_0/k_BT}}{(e^{\hbar\omega_0/k_BT}-1)^2}, \tag{54}$$

with the heat capacity exponentially suppressed at low temperatures, $k_BT \ll \hbar\omega_0$ and exhibiting expected superposition at high temperatures, $k_BT \gg \hbar\omega_0$.

2. Acoustic Debye phonons

Acoustic phonons appear in crystals where Coulomb interactions are well screened, and share a lot in common with the photons in black-body radiation studied in the previous section, with speed of light c replace by the speed of sound c_T and c_L for transvers and longitudinal modes. Their key property is that they are gapless at low momenta, vanishing linearly at $k = 0$, as illustrated in Fig.(12).

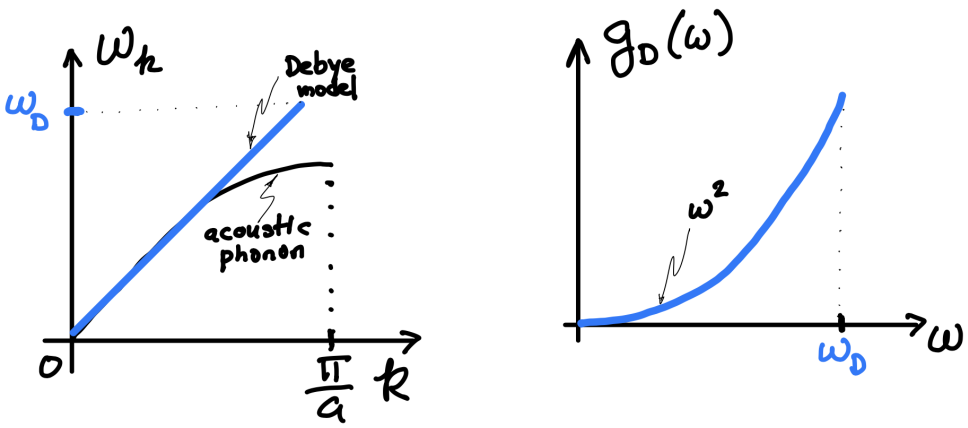

FIG. 12: (a) A dispersion of an acoustic phonon, modeled by a linearly dispersing Debye phonon with $\omega_{k,\alpha} = c_\alpha k$, with two transverse modes at speed c_T and one longitudinal mode at speed c_L. (b) The corresponding density of states for Debye phonons, with $g_D(\omega) \sim \omega^2$ up until the Debye frequency ω_D and then cutoff to zero for $\omega > \omega_D$. A simplest lattice model of Debye phonons is that illustrated in Fig.(10).

For a simplified model of such acoustic phonons we replace the nontrivial dispersion $\omega_{k,\alpha}$ by a linear ones, $\omega_{k,\alpha} = c_\alpha k$, with two transverse modes at speed c_T and one longitudinal mode at speed c_L, as illustrated in Fig.(12), with minor expected errors near the BZ boundary only.

The corresponding density of states of Debye phonon can be straightforwadly evaluated, for $\omega < \omega_D$ (with ω_D yet to be determined) is given by,

$$\begin{aligned} g_D(\omega) &= \sum_{\mathbf{k}\in \text{B.Z.}} \delta(\omega - c_L k) + 2 \sum_{\mathbf{k}\in \text{B.Z.}} \delta(\omega - c_T k) = V \int_{\text{BZ}} \frac{d^3k}{(2\pi)^3} \left[\delta(\omega - c_L k) + 2\delta(\omega - c_T k)\right], \\ &= \frac{V}{2\pi^2} \left[\frac{1}{c_L^3} + \frac{2}{c_T^3}\right] \omega^2, \quad \text{for } \omega < \omega_D, \qquad (55) \\ &= 0, \quad \text{for } \omega > \omega_D, \qquad (56) \end{aligned}$$

illustrated in Fig.(12). We fix the one unknown parameter, Debye maximum frequency, ω_D by requiring that $g_D(\omega)$ satisfies the total number of modes ($3N$) constraint, (53). This gives,

$$\omega_D^3 = 18\pi^2 \frac{N}{V} \left(\frac{1}{c_L^3} + \frac{2}{c_T^3}\right)^{-1},$$

and

$$g_D(\omega) = \frac{9N}{\omega_D^3} \begin{cases} \omega^2, & \text{for } \omega < \omega_D, \\ 0, & \text{for } \omega > \omega_D. \end{cases} \tag{57}$$

With this we then obtain for the Debye heat capacity,

$$C_V(T) = \frac{9Nk_B}{\omega_D^3} \int_0^{\omega_D} d\omega \omega^2 \frac{(\hbar\omega/k_BT)^2 e^{\hbar\omega/k_BT}}{(e^{\hbar\omega/k_BT}-1)^2}, \tag{58}$$

$$= 9Nk_B \left(\frac{k_BT}{\omega_D}\right)^3 \int_0^{\frac{\hbar\omega_D}{k_BT}} dx \frac{x^4 e^x}{(e^x-1)^2}. \tag{59}$$

The heat capacity $C_V(T)$ exhibits two contrasting behaviors as a function of T depending on the value of ω_D. For $k_BT \ll \hbar\omega_D$, one is effectively in the infinite ω_D limit, which allows us to take the upper limit of integration to infinity, and the result reduces to $\sim T^3$, that is qualitatively identical to that of the black-body radiation Stefan-Boltzmann's law, where indeed there is no upper limit on ω.

In contrast, for high temperatures, $k_BT \gg \omega_D$, the upper limit is small enough that exponential regime of the integrand is never explored and it can be expanded to lowest order, giving the expected equipartition form, $C_V(T \gg \hbar\omega_D/k_B) \approx 3Nk_B$.

IV. NONINTERACTING FERMI GAS: ELECTRONS IN A METAL AND PAULI PARAMAGNETISM

In Sec.III we derived general thermodynamics of a noninteracting Fermi gas (along with the Bose gas). We now explore its details, the phenomenology that follows, with the eye to its most important application of electrons in metals. The latter can be modelled as a Fermi gas of electrons confined to a "box" (that, for simplicity we take to have periodic boundary conditions), characterized by single-particle states $\mathbf{k}$. This free electron model of metals was developed in 1927, principally by Arnold Sommerfeld, who combined the classical Drude model with quantum mechanical Fermi-Dirac statistics.

A. Ground state

Much of the phenomenology of simple metals can be captured by ideal Fermi gas. Before turning to thermodynamics, it is of interest to first explore the properties of the many-body ground state, to which the thermodynamics reduces (see below) in the zero-temperature limit.

As discussed in the Introduction, the many-body ground state given by the antisymmetrized product state of single-particle eigenstates - one electron per state according to the Pauli principle, much like filling elecronic levels of a multi-electron atom, that for spinless (e.g., polarized by an external Zeeman field) electrons is given by Eq.(5),

$$\begin{aligned} &\Psi_{\mathbf{k}_1,\ldots,\mathbf{k}_N}(\mathbf{x}_1,\ldots,\mathbf{x}_N) \qquad (60)\\ &= \frac{1}{\sqrt{N!}}\left[\psi_{\mathbf{k}_1}(\mathbf{x}_1)\psi_{\mathbf{k}_2}(\mathbf{x}_2)\ldots\psi_{\mathbf{k}_N}(\mathbf{x}_N)+(-1)^P\psi_{\mathbf{k}_1}(\mathbf{x}_{P1})\psi_{\mathbf{k}_2}(\mathbf{x}_{P2})\ldots\psi_{\mathbf{k}_N}(\mathbf{x}_{PN})+\ldots\right], \end{aligned}$$

with single-electron eigenstates $\psi_{\mathbf{k}}(\mathbf{x})$ for a periodic "box" confinement (i.e., no external potential) given by plane-waves (with $\mathbf{k}=\frac{2\pi}{L}(n_x,n_y,n_z)$). In the second-quantized occupation basis form,

$$|\{n_{\mathbf{k}}\}\rangle \;=\; \prod_{\mathbf{k}}(c_{\mathbf{k}}^{\dagger})^{n_{\mathbf{k}}}|0\rangle, \qquad (61)$$

with occupation numbers $n_{\mathbf{k}}\in 0,1$, and anticommutation relations of the fermionic creation operators $c_{\mathbf{k},}^{\dagger}$ automatically encoding the crucial Pauli principle.

The electron gas ground state (see Fig.13) is then given by occupation of states with the lowest single-particle energies $\epsilon_{\mathbf{k}}$, with 2 electrons $\sigma=\uparrow,\downarrow$ per state in unpolarized case (and 1 electron for the fully polarized case), that we denote as Fermi sea, $|FS\rangle$. For a system with isotropic dispersion, this corresponds to

$$n_{\mathbf{k}} \;=\; \begin{cases} 1, \text{ for } |\mathbf{k}|<k_F, \\ 0, \text{ for } |\mathbf{k}|\geq k_F, \end{cases}, \qquad (62)$$

where total number of atoms N is related to the highest occupied Fermi momentum state

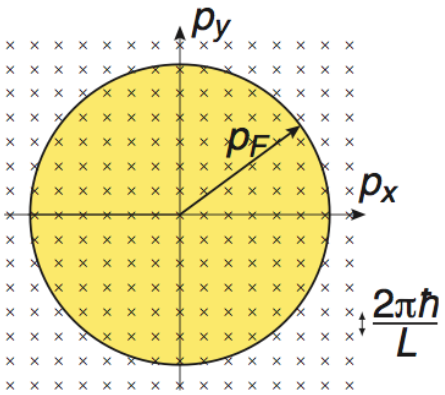

FIG. 13: Ground state of a 2d Fermi gas, with all states with $k < k_F$ filled by electrons (yellow) and empty for $k > k_F$, with one per $\mathbf{k}$ for spinless electrons and two $\uparrow, \downarrow$ for spinful ones. Generalization to arbitrary dimension is obvious with Fermi circle replaced by Fermi hypersphere of radius k_F. The surface of the sphere, defined by $\epsilon_{\mathbf{k}} = \epsilon_F$ is dubbed the Fermi surface.

k_F and Fermi energy $\epsilon_F = \frac{\hbar^2 k_F^2}{2m}$,

$$N = \sum_{\mathbf{k},\sigma} 1 = 2\sum_{\mathbf{k}} 1 = 2L^d \int_0^{k_F} \frac{d^d k}{(2\pi)^d} 1 \equiv 2L^d \int \frac{d^d k}{(2\pi)^d} n_{\mathbf{k}}, \tag{63}$$

$$\equiv \int_0^{\epsilon_F} d\epsilon g(\epsilon), \tag{64}$$

$$= 2L^d C_d k_F^d / d. \tag{65}$$

Above $C_d \equiv S_d/(2\pi)^d$ and $S_d = 2\pi^{d/2}/\Gamma(d/2)$ is the surface area of a $d-1$ dimensional unit sphere, $S_1 = 2, S_2 = 2\pi, S_3 = 4\pi$ and $g(\epsilon) = C_d \left(\frac{2m}{\hbar^2}\right)^{d/2} \epsilon^{d/2-1} =_{3d} \frac{1}{2\pi^2} \left(\frac{2m}{\hbar^2}\right)^{3/2} \epsilon^{1/2} = \frac{3}{2} n(\epsilon)/\epsilon$ is the density of states. Consistent with dimensional analysis, above expresses the density n in terms of the Fermi momentum and Fermi energy, $n \sim k_F^d \sim \epsilon_F^{d/2}$, with 3d case $n_{3d} = \frac{k_F^3}{3\pi^2}$. As we will find below, above is the "number" equation from thermodynamics, evaluated at $T = 0$, where it is simply the ground state expression.

The total ground state energy and pressure are then given by

$$E_{GS} = \sum_{\mathbf{k},\sigma} \frac{\hbar^2 k^2}{2m} = 2\sum_{\mathbf{k}} \epsilon_{\mathbf{k}} n_{\mathbf{k}} = 2L^d \int_0^{k_F} \frac{d^d k}{(2\pi)^d} \frac{\hbar^2 k^2}{2m} = \frac{d}{d+2} N\epsilon_F =_{d=3} \frac{3}{5} N\epsilon_F, \tag{66}$$

$$P = -\frac{\partial E}{\partial V}|_N = \frac{2}{d+2} n\epsilon_F =_{d=3} \frac{2}{5} n\epsilon_F. \tag{67}$$

Thus for metals, even at zero temperature the energy and pressure are nonzero and in fact

extremely high, all a consequence of uncompromising Pauli exclusion principle. As a result the electrons in a metal are moving at extremely high velocity with Fermi velocity, $v_F \sim 10^6$ m/sec and Fermi temperature $T_F \sim 10^4$ Kelvin.

B. Thermodynamics

As discussed and studied in general in Sec.III the thermodynamics is conveniently computed in the grand-canonical ensemble, encoded by the grand-canonical partition function

$$\begin{aligned} \mathcal{Z} &= \mathrm{Tr} e^{-\beta(\hat{H}-\mu\hat{N})} = \sum_{\{n_{\mathbf{k}\sigma}\}} e^{-\beta\sum_{\mathbf{k}\sigma}(\epsilon_k-\mu)n_{\mathbf{k}\sigma}}, & (68)\\ &= \prod_{\mathbf{k}\sigma}\left(\sum_{n_{\mathbf{k}\sigma}} e^{-\beta(\epsilon_k-\mu)n_{\mathbf{k}\sigma}}\right), & (69)\\ &= \prod_{\mathbf{k}\sigma}\left(1+e^{-\beta(\epsilon_k-\mu)}\right), & (70)\end{aligned}$$

which gives the grand-canonical free energy

$$\begin{aligned} \mathcal{F} &= -k_BT\ln\mathcal{Z} = -k_BT\sum_{\mathbf{k}\sigma}\ln\left(1+e^{-\beta(\epsilon_k-\mu)}\right), & (71)\\ &= -k_BTL^d\int d\epsilon g(\epsilon)\ln\left(1+e^{-\beta(\epsilon-\mu)}\right), & (72)\end{aligned}$$

and also the pressure through $PV = -\mathcal{F}$. With this, we can also calculate the total number of particles (or equivalently density n) as a function of chemical potential and temperature

$$N = -\frac{\partial\mathcal{F}}{\partial\mu} = \sum_{\mathbf{k},\sigma}\frac{1}{e^{\beta(\epsilon_k-\mu)}+1} \equiv \sum_{\mathbf{k},\sigma}\langle n_{\mathbf{k}\sigma}\rangle, \quad (73)$$

where the average occupation function of the single-particle states $\mathbf{k}$ is the Fermi-Dirac distribution,

$$\langle n_{\mathbf{k}\sigma}\rangle = \frac{1}{e^{\beta(\epsilon_k-\mu)}+1} \equiv n_F(\epsilon_k) \equiv f(\epsilon_k) \approx \begin{cases} e^{-\beta(\epsilon_k-\mu)}, & \text{for } \mu \ll k_BT, \text{ nondegenerate,} \\ \theta(\mu-\epsilon_k), & \text{for } \mu \gg k_BT, \text{ degenerate,}\end{cases}$$

illustrated below. The average occupation $\langle n_{\mathbf{k}\sigma}\rangle$ can also be computed more directly via

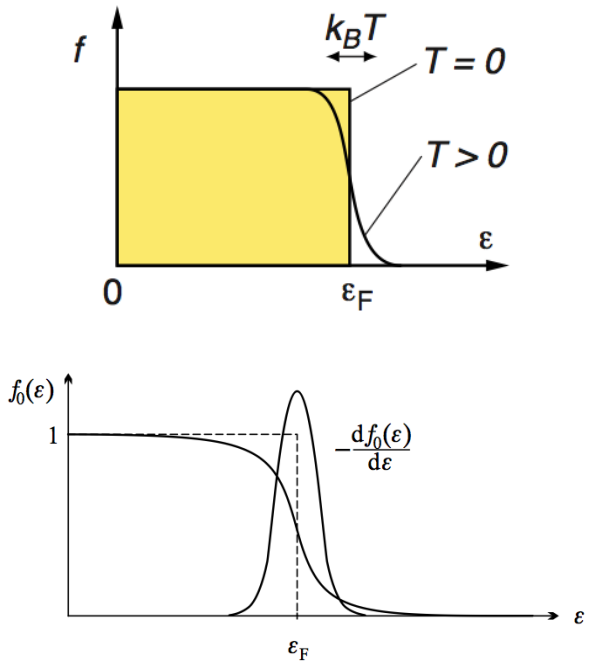

FIG. 14: Fermi-Dirac distribution describing finite T momentum states occupation in the noninteracting Fermi gas and the corresponding derivative.

$$\langle \hat{n}_{\mathbf{k}\sigma} \rangle = \frac{1}{Z_{gr}} \mathrm{Tr} \left(\hat{n}_{\mathbf{k}\sigma} e^{-\beta \hat{H}_\mu} \right).$$

We note that the low T limit of $n_F(\epsilon_k)$ given by the step function then in $T \to 0$ limit exactly reproduces the results of the ground state analysis in the previous subsection, as expected.

Using $n_F(\epsilon_k)$ and the density of states to perform the sum in the thermodynamic limit, we obtain

$$N = V \int_0^\infty d\epsilon g(\epsilon) n_F(\epsilon), \tag{74}$$

$$= \frac{V}{2\pi^2} \left(\frac{2m}{\hbar^2} \right)^{3/2} \int_0^\infty d\epsilon \epsilon^{1/2} n_F(\epsilon) = 2V \left(\frac{mk_BT}{2\pi\hbar^2} \right)^{3/2} f_{1/2}(\mu/k_BT), \tag{75}$$

where

$$f_{1/2}(x) = \frac{2}{\sqrt{\pi}} \int_0^\infty \frac{\epsilon^{1/2} d\epsilon}{e^{\epsilon - x} + 1}$$

(the analogue of $g_\nu(z)$ we introduced for bosons in earlier sections) is the order 1/2 Fermi integral that can be evaluated numerically. Using $f_j(x \to -\infty) \to e^x$, in the classical limit of $e^{\mu/k_BT} \ll 1$, we recover the classical Boltzmann gas result $n = 2 \left(\frac{mk_BT}{2\pi\hbar^2} \right)^{3/2} e^{\mu/k_BT}$, giving

$\mu \approx -k_B T \ln[1/(n\lambda_T^3)] \sim -T \ln T$ (λ_T is thermal deBroglie wavelength, that in the classical limit is much smaller than interparticle spacing).

In the opposite limit $\mu/k_B T \gg 1$ relevant to metals, we utilize large x expansion, $f_{1/2}(x) \approx \frac{4}{3\sqrt{\pi}} x^{3/2} \left(1 + \frac{\pi^2}{8x^2} + \ldots\right)$, obtaining

$$n = \frac{1}{3\pi^2} \left(\frac{2m\mu}{\hbar^2}\right)^{3/2} \left(1 + \frac{\pi^2}{8} \left(\frac{k_B T}{\mu}\right)^2 + \ldots\right),$$

that by definition of the Fermi energy (derived in sections above) is also given by $n = \frac{1}{3\pi^2} \left(\frac{2m\epsilon_F}{\hbar^2}\right)^{3/2}$, consistent with $\mu(T=0) = \epsilon_F$ and giving

$$\mu = \epsilon_F \left[1 - \frac{\pi^2}{12} \left(\frac{k_B T}{\epsilon_F}\right)^2 \ldots\right].$$

We can understand this weak reduction of μ with increasing T by noting (see Fig.(14)) that for fixed μ the area under the curve (including the $\epsilon^{1/2}$ density of states factor) *increases* with T broading: although to lowest order the decrease from rounding below μ is compensated by a tail above μ, low ϵ is cutoff at $\epsilon = 0$, while high ϵ tail extends to infinity. Thus to keep the electron number fixed at N, the chemical potential, $\mu(T)$ must *decrease* with increasing T to compensate this excited electron-hole imbalance.

The energy and heat capacity are also straightforwardly computed either directly or through the derivative of the free-energy, giving

$$E = 2 \sum_{\mathbf{k}} \epsilon_k f(\epsilon_k), \tag{76}$$

$$C_{el} = \frac{\partial E}{\partial T}, \tag{77}$$

for $T = 0$ reducing to results obtained in previous subsection. We leave a detailed evaluation of these as a homework exercise, only quoting the 3d $T \to 0$ limit result

$$c_{el} \equiv C_{el}/V = \frac{\pi^2}{3} g(\epsilon_F) k_B^2 T \equiv \gamma T,$$

where γ is referred to as the Sommerfeld coefficient, and $g(\epsilon_F) \sim n/\epsilon_F \sim \epsilon_F^{d/2-1}$.

The full result is illustrated in Fig.(15), interpolating betweent the high-temperature

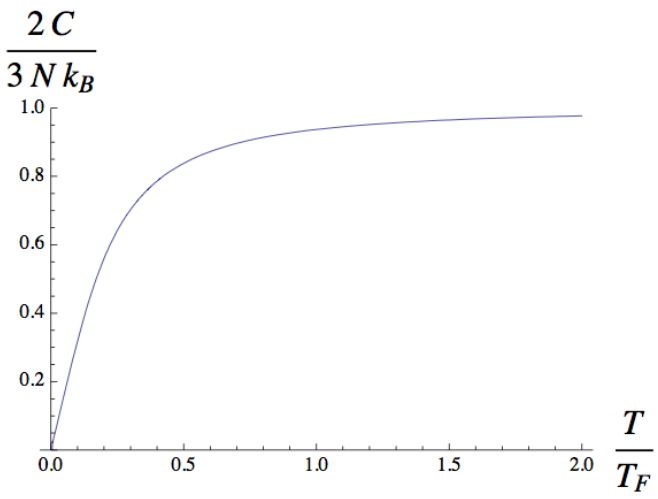

FIG. 15: Electronic heat capacity $C_{el}(T)$, interpolating betweent the high temperature classical equipartition result of $\frac{1}{2}dNk_B$ and the low-T result γT one.

classical equipartition result of $\frac{1}{2}dNk_B$ and the low-T result above. In interacting systems γ is substantially different form above free electron gas, with the difference attributed to the effective mass increase due to interactions. This general *linear* T equipartition-violating heat-capacity, that is hallmark of simple metals and Fermi gases and liquids in general - a truimph of the Sommerfeld theory - is a direct consequence of the Pauli principle arising from the existence of a Fermi surface (where the low-energy excitations contributing to C_v are residing). It can be understood as effective equipartition but with the number of degrees of freedom, $N_{\rm dof}(T) \sim Nk_BT/\epsilon_F = NT/T_F$, of the low-energy fermionic excitations around the Fermi surface being temperature dependent. Only a small fraction $k_BT/\epsilon_F \ll 1$ of the Fermi sea close to the Fermi surface can participate in excitations, with others Pauli blocked. This small fraction of electrons then equipartitions the thermal energy, thereby giving

$$E_{excitation} \approx N\left(\frac{k_BT}{\epsilon_F}\right)k_BT,$$

whose derivative leads to the linear T dependence (rather than the constant classical Nk_B result) of simple metals, quoted above. We note that unlike bosons of the previous sections, this fermionic linear in T heat capacity is dimension independent.

A systemmatic general analysis of the low-temperature behavior of any electronic quantities can be obtained using the so-called Sommerfeld expansion, which relies on the sharpness of the derivative of the Fermi-Dirac distribution function at low T. Namely, integrating by

parts to bring out the sharp feature of the FD distribution at low T, for a generic average we obtain

$$\langle H\rangle = \int_{-\infty}^{\infty} d\epsilon H(\epsilon) f(\epsilon), \tag{78}$$

$$= \int_{-\infty}^{\infty} d\epsilon \left(\int_{-\infty}^{\mu+(\epsilon-\mu)} H(\epsilon') d\epsilon' \right) \frac{\partial f}{\partial \mu}, \tag{79}$$

which can then Taylor expanded in $\epsilon - \mu \approx O[(k_B T/\epsilon_F)^2]$.

Having established the basics of the *noninteracting* Fermi gas, we next turn to its response to an external magnetic field for the spin-full Fermi gas (still ignoring interactions), namely the so-called Pauli itinerant paramagnet.

C. Pauli paramagnetism

As we have seen above, the ground state of a noninteracting Fermi gas is nonmagnetic, with spin up and down states equally populated. It is thus a quantum itinerate (spins are not fixed on ions but are carried by the electron liquid) paramagnet. On general grounds we therefore expect that in the presence of an external magnetic field these spin states will be split by the eigenvalues of the Zeeman energy,

$$H_Z = -\boldsymbol{\mu} \cdot \mathbf{B} = \frac{g\mu_B}{\hbar} \mathbf{S} \cdot \mathbf{B} = \mu_B B \sigma_z,$$

$\epsilon_{\uparrow,\downarrow} = \pm \mu_B B$. Ignoring orbital effects of the magnetic field (that lead to the Landau diamagnetism of orbital currents generating magnetic moments), together with the kinetic energy the single-electron spectrum is then given by

$$\epsilon_{\mathbf{k}\sigma} = \frac{\hbar^2 k^2}{2m} + \sigma \mu_B B, \quad \sigma = \pm 1.$$

As before we determine the chemical potential $\mu(n, T, B)$ through the constraint on the

total electron number density $n = N/V$

$$n = n_\downarrow + n_\uparrow = V^{-1}\sum_{\mathbf{k}} f(\epsilon_{\mathbf{k}\downarrow}) + V^{-1}\sum_{\mathbf{k}} f(\epsilon_{\mathbf{k}\uparrow}), \tag{80}$$

$$= \int_{-\mu_B B}^{\infty} d\epsilon g(\epsilon + \mu_B B) f(\epsilon) + \int_{\mu_B B}^{\infty} d\epsilon g(\epsilon - \mu_B B) f(\epsilon), \tag{81}$$

$$\tag{82}$$

The spin magnetization response (in the absence of orbital effects) is simply the difference between $n_\uparrow, n_\downarrow$ densities

$$m = \mu_B \int_{-\mu_B B}^{\infty} d\epsilon g(\epsilon + \mu_B B) f(\epsilon) - \mu_B \int_{\mu_B B}^{\infty} d\epsilon g(\epsilon - \mu_B B) f(\epsilon), \tag{83}$$

$$= \mu_B \int_0^{\infty} d\epsilon g(\epsilon) \left[f(\epsilon - \mu_B B) - f(\epsilon + \mu_B B) \right], \tag{84}$$

$$\approx 2\mu_B^2 B \int_0^{\infty} d\epsilon g(\epsilon) \frac{-\partial f(\epsilon)}{\partial \epsilon} = 2\mu_B^2 g(\epsilon_F) B, \quad \text{for } \mu_B B \ll \epsilon_F, \quad T \to 0, \tag{85}$$

where the last expression is evaluated in the weak B linear response, $T = 0$ limit, utilizing δ-function form of the derivative of the Fermi-Dirac distribution.

Above coupled integrals can be computed numerically, giving the full expression for $m(n, T, B)$ after using $\mu(n, T, B)$ from the number equation. At $T = 0$, the full magnetization can be straightforwardly calculated analytically using $f_{T=0}(x) = \theta(\epsilon_F - x)$,

$$m = \mu_B \left[\int_{-\mu_B B}^{\epsilon_F} d\epsilon g(\epsilon + \mu_B B) - \int_{\mu_B B}^{\epsilon_F} d\epsilon g(\epsilon - \mu_B B) \right], \tag{86}$$

$$= \mu_B c_d \int_{\epsilon_F - \mu_B B}^{\epsilon_F + \mu_B B} d\epsilon \, \epsilon^{d/2-1} = \mu_B c_d \frac{2}{d} \left[(\epsilon_F + \mu_B B)^{d/2} - (\epsilon_F - \mu_B B)^{d/2} \right], \tag{87}$$

$$\approx \chi_{Pauli} B, \quad \text{for } B \to 0 \tag{88}$$

where density of states $g(\epsilon) = c_d \epsilon^{d/2-1}$ was used with overall constants packaged into c_d, finding Pauli linear susceptibility

$$\chi_{Pauli} = \frac{d}{2} \frac{n\mu_B^2}{\epsilon_F} = 2\mu_B^2 g(\epsilon_F), \tag{89}$$

to be compared to the Curie susceptibility $\chi_{Curie} \sim \frac{\mu_B^2}{k_B T}$ (that we derived for noninteracting local moments), with the role of $k_B T$ replaced by ϵ_F. As with the qualitative discussion

of the low-temperature excitation energy and the heat capacity, above, here too we can understand the result of the temperature-independent Pauli susceptibility in terms of Curie susceptibility of the reduced, temperature dependent number of excitations confined by the Pauli principle to the k_BT/ϵ_F shell around the Fermi surface. This reproduces the detailed result via

$$\chi_{Pauli} \sim \frac{k_BT}{\epsilon_F}\chi_{Curie} = \frac{k_BT}{\epsilon_F}\frac{\mu_B^2}{k_BT} = \frac{\mu_B^2}{\epsilon_F}.$$

The Wilson ratio (K.G. Wilson, 1975) for a free electron gas is therefore given by

$$R_W \equiv \frac{\chi_P T}{c_{el}} = \frac{3}{\pi^2}\left(\frac{\mu_B}{k_B}\right)^2.$$

A substantial deviation (e.g., even a factor of 2) of R_W from above ideal value is usually attributed to strong electron-electron correlations.

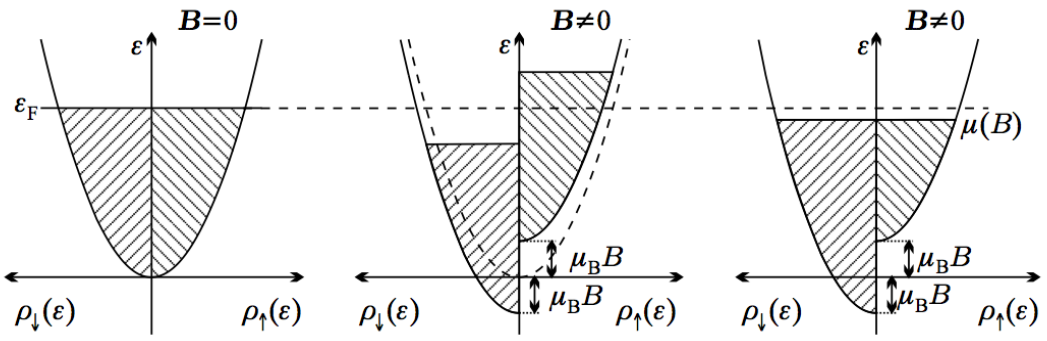

FIG. 16: The electronic density of states for the two spin orientations, in the absence a magnetic field (left) and in its presence, before spin-flip and spin-transfer equilibration processes take place (middle) and in thermal equilibrium (right).

Above we have focussed on magnetic response to an external field due to spins, ignoring orbital effects of charged electrons.

D. Landau diamagnetism

In addition to the Zeeman spin effect, $H_{Zeeman} = \frac{g\mu_B}{\hbar}\mathbf{S}\cdot\mathbf{B}$ of an external magnetic field analyzed above, electrons are charged particles and so respond to orbital effects of the magnetic field by executing Larmor orbits, due to Lorentz force, resulting in circulating currents that contribute to magnetization m. According to the Bohr-Van-Leeuwen theorem, within

purely classical statistical mechanical treatment there is no orbital magnetism. However, within a quantum treatment, indeed orbital response to a magnetic field is diamagnetic with the (so-called) Landau susceptibility for free electrons given by

$$\chi_{Landau} = -\frac{1}{3}\chi_{Pauli}, \tag{90}$$

i.e., exactly 1/3 of the Pauli paramagnetic susceptibility.

E. Degeneracy pressure

Above analysis of metals extends to any collection of noninteracting fermions, with another important application of electrons comprising a white dwarf and neutrons comprising a neutron star.

In a white dwarf, the gravitational energy $E_G \sim GM^2 n(r)/r$ in equilibrium ($dP/dr = nF_G(r)$) gives $P_G \sim GM^2/r^4 \sim GM^2 n^{4/3}$, driving to collapse the white dwarf, which for not too large M is prevented by the electron degeneracy pressure $P_P = n\epsilon_F \sim n^{5/3}$, calculated above. Since $5/3 > 4/3$, the Pauli pressure can support the star from its gravitational collapse. However, for sufficiently large pressure, (which happens for $M > 1.5M_{\rm solar}$, the Chandrasekhar limit) the energetics changes, electrons fuse with protons to make neutrons, converting the white dwarf into a neutran star.

The resulting neutron star is then supported by the degeneracy pressure of the neutrons against its gravitational collapse. For sufficiently high pressure, the energetic switches to relativistic one with dispersion $p^2/2m \to pc$. This changes the neutrons' degeneracy pressure to $P_P = ncp_F \sim n^{4/3}$, which can no longer support the gravitational forces of the neutron star. It then collapses and explodes in a supernova, potentially leading to a black hole.

V. CONCLUSION

With this lecture discussion, amplified by your detailed homeowork analysis we now understand the detailed role of quantum statistics of bosons and fermions in many-body quantum statistical mechanics and its drastic manifestations in their corresponding phenomenology in the degenerate regime of low $T < T_*$. In the next set of lectures we will move beyond noninteracting many-body systems and focussing first on magnetic systems

study striking role of spin exchange interactions that lead to phase transitions to e.g., a ferromagnetic state, as well as other types of phase transitions.

---

[1] Pathria: *Statistical Mechanics*, Butterworth-Heinemann (1996).

[2] L. D. Landau and E. M. Lifshitz: *Statistical Physics*, Third Edition, Part 1: Volume 5 (Course of Theoretical Physics, Volume 5).

[3] Mehran Kardar: *Statistical Physics of Particles*, Cambridge University Press (2007).

[4] Mehran Kardar: *Statistical Physics of Fields*, Cambridge University Press (2007).

[5] J. J. Binney, N. J. Dowrick, A. J. Fisher, and M. E. J. Newman : *The Theory of Critical Phenomena*, Oxford (1995).

[6] John Cardy: *Scaling and Renormalization in Statistical Physics*, Cambridge Lecture Notes in Physics.

[7] P. M. Chaikin and T. C. Lubensky: *Principles of Condensed Matter Physics*, Cambridge (1995).

[8] "Chaos and Quantum Thermalization", Mark Srednicki, *Phys. Rev. E* **50** (1994); arXiv:cond-mat/9403051v2; "The approach to thermal equilibrium in quantized chaotic systems", *Journal of Physics A* **32**, 1163 (1998).

[9] "Quantum statistical mechanics in a closed system", J. M. Deutsch, *Phys. Rev. A* **43**, 2046.

[10] J. Bartolome, et al., *Phys. Rev. Lett.* **109**, 247203 (2012).

[11] D. M. Basko, I. L. Aleiner and B. L. Altshuler, *Annals of Physics* **321**, 1126 (2006).

[12] "Many body localization and thermalization in quantum statistical mechanics", R. Nandkishore, D. Huse, *Annual Review of Condensed Matter Physics* **6**, 15-38 (2015).

[13] D. Arovas, "Lecture Notes on Magnetism" and references therein. see "Magnetism" Boulder School Lectures at http://boulder.research.yale.edu/Boulder-2003/index.html

[14] *Quantum Mechanics and Path Integrals*, R. P. Feynman and A. R. Hibbs.

[15] *Statistical Mechanics Lectures'*, R. P. Feynman.

[16] *Bose-Einstein Condensation*, by A. Griffin, D. W. Snoke, S. Stringari.